

**Energy deposition in hard dihadron triggered events in heavy-ion collisions**

Thorsten Renk\*

*Department of Physics, P. O. Box 35 FI-40014, University of Jyväskylä, Finland and Helsinki Institute of Physics, P. O. Box 64 FI-00014, University of Helsinki, Finland*

(Received 8 April 2008; published 11 July 2008)

The experimental observation of hadrons correlated back-to-back with a (semi-)hard trigger in heavy-ion collisions has revealed a splitting of the away side correlation structure in a low to intermediate transverse momentum ( $P_T$ ) regime. This is consistent with the assumption that energy deposited by the away side parton into the bulk medium produced in the collision excites a sonic shock wave (a Mach cone) that leads to away side correlation strength at large angles. A prediction that follows from assuming such a hydrodynamical origin of the correlation structure is that there is a sizable elongation of the shock wave in rapidity due to the longitudinal expansion of the bulk medium. Using a single-hadron trigger, this cannot be observed because of the unconstrained rapidity of the away side parton. Using a dihadron trigger, the rapidity of the away side parton can be substantially constrained and the longitudinal structure of the away side correlation becomes accessible. However, in such events several effects occur that change the correlation structure substantially: There is not only a sizable contribution due to the fragmentation of the emerging away side parton but also a systematic bias toward small energy deposition into the medium and hence a weak shock wave. In this article, both effects are addressed.

DOI: [10.1103/PhysRevC.78.014903](https://doi.org/10.1103/PhysRevC.78.014903)

PACS number(s): 25.75.Gz

**I. INTRODUCTION**

The experimental observation of hadrons correlated back-to-back with a hard or semihard trigger hadron in Au-Au collisions at 200 A GeV has revealed a splitting of the away side correlation peak in a semihard momentum regime between 1 and 2.5 GeV [1–4] that is absent in p-p collisions where two back-to-back peaks appear. This means that the main strength of the away side correlation in Au-Au collisions in this momentum region is not found in the direction of the away side parton but at a large angle with respect to it. This angle is found to remain constant if the trigger momentum is changed and also for a variety of associate hadron momenta in the semihard regime. This observation can be contrasted with back-to-back correlations at hard trigger and associate hadron momenta well above 4 GeV [5] that show a reappearance of back-to-back correlations as seen in p-p collisions, albeit suppressed.

This pattern has given rise to the idea that while energy loss of a back-to-back parton pair is responsible for the suppression observed at high  $P_T$ , the measurements at intermediate associate hadron  $P_T$  show how this energy is redistributed into the medium and may in fact show the recoil of the medium in the form of a hydrodynamical shock wave [6]. Phenomenological comparisons of this scenario with the data using the same Monte Carlo (MC) simulation for energy loss and energy redistribution in shock waves found agreement with both the high  $P_T$  correlation pattern [7,8] and the low  $P_T$  peak splitting [9]. A comparison with the measured three-particle correlations [10] has also been made in the same framework [11], but remains somewhat inconclusive as to prove or disprove the existence of shock waves as the chief

mechanism for energy redistribution. However, in Ref. [12] an important difference between sonic shock waves and other conical emission mechanisms has been pointed out, i.e., the longitudinal elongation of the shock cone due to longitudinal flow that should result in a large extension of the correlation signal in rapidity for a hydrodynamical excitation of the medium.

This elongation is obscured in single-hadron triggered correlation measurements due to the fact that the rapidity of the away side parton is not determined by the rapidity of the trigger hadron and all possible rapidities of the away side parton have to be averaged. However, if the trigger is a sufficiently hard back-to-back hadron pair, then the rapidity position of the away side parton is very constrained and the elongation should be observable. Unfortunately, requiring a hard trigger hadron on the away side introduces a bias toward small energy deposition into the medium. In addition, an away side parton emerging from the medium produces not only the leading away side hadron (which is part of the trigger) but also subleading hadrons building up correlation strength along the jet axis also at intermediate  $P_T$ , thus obscuring any large-angle signal of a shock wave by filling in the dip between the shock wave wings with a back-to-back peak. In this article, we aim at a discussion of these effects.

**II. THE MODEL**

We simulate hard back-to-back hadron production in a MC model. There are three important building blocks to this computation: (1) the primary hard parton production, (2) the propagation of the partons through the medium, and (3) the hadronization of the partons. Only step (2) probes properties of the medium, and hence it is here that we must specify details of the evolution of the medium and of the parton-medium

\*trenk@phys.jyu.fi

interaction. The model is described in great detail in Refs. [8] and [13]; here we just provide a short overview.

### A. Primary parton production

The production of two hard partons,  $k, l$ , in leading order (LO) perturbative Quantum Chromodynamics (pQCD) is described by

$$\frac{d\sigma^{AB \rightarrow kl+X}}{dp_T^2 dy_1 dy_2} = \sum_{ij} x_1 f_{i/A}(x_1, Q^2) x_2 f_{j/B}(x_2, Q^2) \frac{d\hat{\sigma}^{ij \rightarrow kl}}{d\hat{t}}, \quad (1)$$

where  $A$  and  $B$  stand for the colliding objects (protons or nuclei) and  $y_{1(2)}$  is the rapidity of parton  $k(l)$ . The distribution function of a parton type  $i$  in  $A$  at a momentum fraction  $x_1$  and a factorization scale  $Q \sim p_T$  is  $f_{i/A}(x_1, Q^2)$ . The distribution functions are different for the free protons [14,15] and nucleons in nuclei [16,17]. The fractional momenta of the colliding partons  $i, j$  are given by  $x_{1,2} = \frac{p_T}{\sqrt{s}}(\exp[\pm y_1] + \exp[\pm y_2])$ .

Expressions for the pQCD subprocesses  $\frac{d\hat{\sigma}^{ij \rightarrow kl}}{d\hat{t}}(\hat{s}, \hat{t}, \hat{u})$  as a function of the parton Mandelstam variables  $\hat{s}, \hat{t}$ , and  $\hat{u}$  can be found, e.g., in Ref. [18]. By selecting pairs of  $k, l$  while summing over all allowed combinations of  $i, j$ , i.e.,  $gg, gq, g\bar{q}, qq, q\bar{q}, \bar{q}q$ , where  $q$  stands for any of the quark flavors  $u, d, s$ , we find the relative strength of different combinations of outgoing partons as a function of  $p_T$ .

For the present investigation, we consider a dihadron trigger at midrapidity  $y_1 = y_2 = 0$ . By MC sampling Eq. (1) we generate a back-to-back parton pair with given parton types and flavors at transverse momentum  $p_T$ . To account for various effects, including higher order pQCD radiation, transverse motion of partons in the nucleon (nuclear) wave function and effectively also the fact that hadronization is not a collinear process, we fold into the distribution an intrinsic transverse momentum  $k_T$  with a Gaussian distribution of width 1.6 GeV. This momentum vector points in a random direction in the transverse plane and modifies the transverse momenta  $p_{T1}, p_{T2}$  of the outgoing partons in creating a momentum imbalance between them according to  $p_{T1} + p_{T2} = k_T$ .

### B. Parton propagation through the medium

The probability density  $P(x_0, y_0)$  for finding a hard vertex at the transverse position  $\mathbf{r}_0 = (x_0, y_0)$  and impact parameter  $\mathbf{b}$  is given by the product of the nuclear profile functions as

$$P(x_0, y_0) = \frac{T_A(\mathbf{r}_0 + \mathbf{b}/2)T_A(\mathbf{r}_0 - \mathbf{b}/2)}{T_{AA}(\mathbf{b})}, \quad (2)$$

where the thickness function is given in terms of the Woods-Saxon nuclear density  $\rho_A(\mathbf{r}, z)$  as  $T_A(\mathbf{r}) = \int dz \rho_A(\mathbf{r}, z)$ . For the present study, we evaluate Eq. (2) at  $\mathbf{b} = 0$  corresponding to central collisions. Rotating the coordinate system such that the near side parton propagates in the  $(-x)$  direction, the path of a given parton through the medium  $\xi(\tau)$  is determined by its primary vertex  $\mathbf{r}_0$  and we can compute the energy loss probability  $P(\Delta E)_{\text{path}}$  for this path. We do this in a radiative

energy loss picture [19,20] by evaluating the line integrals

$$\omega_c(\mathbf{r}_0) = \int_0^\infty d\xi \xi \hat{q}(\xi) \quad \text{and} \quad \langle \hat{q}L \rangle(\mathbf{r}_0) = \int_0^\infty d\xi \hat{q}(\xi) \quad (3)$$

along the path where we assume the relation

$$\hat{q}(\xi) = K \cdot 2 \cdot \epsilon^{3/4}(\xi)(\cosh \rho - \sinh \rho \cos \alpha) \quad (4)$$

between the local transport coefficient  $\hat{q}(\xi)$  (specifying the quenching power of the medium), the energy density  $\epsilon$ , and the local flow rapidity  $\rho$  with angle  $\alpha$  between the flow and parton trajectory [21].  $\epsilon$  and  $\rho$  are taken from medium evolution models [23,24] as discussed in Ref. [8].

$\omega_c$  is the characteristic gluon frequency, setting the scale of the energy loss probability distribution, and  $\langle \hat{q}L \rangle$  is a measure of the path-length weighted by the local quenching power. We view the parameter  $K$  as a tool to account for the uncertainty in the selection of  $\alpha_s$  and possible nonperturbative effects increasing the quenching power of the medium (see discussion in Ref. [7]) and adjust it such that pionic  $R_{AA}$  for central Au-Au collisions is described.

Using the numerical results of [22], we obtain  $P(\Delta E; \omega_c, R)_{\text{path}}$  for  $\omega_c$  and  $R = 2\omega_c^2 / \langle \hat{q}L \rangle$  for given jet production vertex and angle  $\phi$ . In the MC simulation, we first sample Eq. (2) to determine the vertex of origin. We then propagate both partons through the medium evaluating Eqs. (3) and use the output to determine  $P(\Delta E; \omega_c, R)_{\text{path}}$ , which we sample to determine the actual energy loss of both partons in the event.

### C. Hadronization

Finally, we convert the simulated partons into hadrons, provided that a back-to-back pair emerges from the medium after energy loss. More precisely, to determine if there is a trigger hadron above a given threshold, given a parton  $k$  with momentum  $p_T$ , we need to sample  $A_1^{k \rightarrow h}(z_1, p_T)$ , i.e., the probability distribution to find a hadron  $h$  from the parton  $k$ , where  $h$  is the most energetic hadron of the shower and carries the momentum  $P_T = z_1 \cdot p_T$ .

In previous works [7,8] we have approximated this by the normalized fragmentation function  $D_{k \rightarrow h}(z, p_T)$ , sampled with a lower cutoff  $z_{\text{min}}$  that is adjusted to the reference d-Au data. This procedure can be justified by noting that only one hadron with  $z > 0.5$  can be produced in a shower; thus, above  $z = 0.5$  the  $D_{k \rightarrow h}(z, p_T)$  and  $A_1^{k \rightarrow h}(z_1, p_T)$  are (up to the scale evolution) identical, and only in the region of low  $z$  where the fragmentation function describes the production of multiple hadrons do they differ significantly.

We improve on these results by extracting  $A_1(z_1, p_T)$  from the shower evolution code HERWIG [25]. The procedure is described in detail in Ref. [13]. Sampling  $A_1(z_1, p_T)$  for any parton that emerged with sufficient energy from the medium provides the energy of the two most energetic hadrons on both sides of the event. The harder of these two defines the near side. The hadron opposite to it is then the leading away side hadron. For the present investigation, we require both to be in given momentum windows to count a dihadron triggered event. We average the energy loss on near and away side parton over

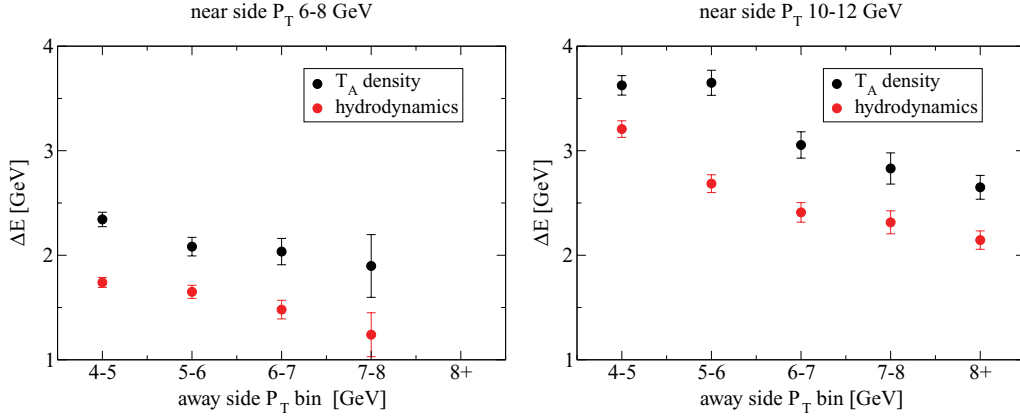


FIG. 1. (Color online) Average energy deposition on the away side for different dihadron trigger momentum ranges in 200 A GeV central Au-Au collisions. The left side shows 6–8 GeV momentum for the hardest hadron; the right side shows 10–12 GeV. The  $x$ -axis shows different bins for the away side hadron momentum; the  $y$ -axis shows the corresponding energy deposition for two different models of the medium evolution (see Ref. [8] for details).

many such events to determine the average energy deposition into the medium.

To compute the correlation strength associated with sub-leading fragmentation of a parton emerging from the medium we evaluate  $A_2(z_1, z_2, p_T)$  (also extracted from HERWIG), the conditional probability to find the second most energetic hadron at momentum fraction  $z_2$  given that the most energetic hadron was found with fraction  $z_1$ . This contribution to the strength of the away side correlation is competing with the shock wave signal.

Our way of modeling hadronization corresponds to an expansion of the shower development in terms of a tower of conditional probability densities  $A_N(z_1, \dots, z_n, \mu)$  with the probability to produce  $n$  hadrons with momentum fractions  $z_1, \dots, z_n$  from a parton with momentum  $p_T$  being  $\prod_{i=1}^n A_i(z_1, \dots, z_i, p_T)$ . Taking the first two terms of this expansion is justified as long as we are interested in sufficiently hard correlations. However, in the following we also consider situations in which the near side trigger momentum is rather hard  $O(10)$  GeV and the away side trigger momentum is likewise hard  $O(5)$  GeV, but with a substantial gap between near and away sides to allow for energy deposition in the medium, but observe fragmentation yield associated with this trigger in a regime where hydrodynamics is valid, i.e.,  $O(1)$  GeV. Because the dihadron trigger forces the parton to high momenta, multihadron production at the low associate scale is likely. Consequently, we have to include the next terms in the expansion. A detailed numerical treatment is very complicated; however, we estimate the next two terms as

$$A_3(z_1, z_2, z_3, p_T) \approx A_2(z_1 + z_2, z_3, p_T) \theta(z_2 - z_3) \quad (5)$$

and

$$A_4(z_1, z_2, z_3, z_4, p_T) \approx A_2(z_1 + z_2 + z_3, z_4, p_T) \times \theta(z_2 - z_3) \theta(z_3 - z_4). \quad (6)$$

This procedure explicitly guarantees energy-momentum conservation and preserves the correct ordering in hadron momenta inside the jet. For the results quoted in the following,

we have verified that the results converge and that  $A_4$  is only a correction and that hence the inclusion of further terms does not alter the result substantially.

### III. RESULTS

In Fig. 1 we show the away side energy deposition into the medium created in central Au-Au collisions at 200 A GeV as a function of the trigger momenta on near and away sides for two different medium evolution models, a hydrodynamical code [23], in the following called “hydrodynamics,” and a parametrized evolution model [24], in the following referred to as “ $T_A$  density” (a longer discussion and contour plots of the evolution of these density evolution models can be found in Ref. [8]). This is the energy available to excite a shock wave. Note that according to the phenomenological analysis [9,11,12] a large fraction  $f = 0.75$  (but not all) of the available energy actually excites a shock wave.

The energy deposition is always largest when the gap between near side and away side trigger momentum is maximal. There is some dependence on what model for the medium evolution is assumed to be valid; however, some general trends remain robust: The energy deposition is roughly a third of the highest (near side) trigger energy. The additional variation with the away side  $P_T$  is about 50%.

On the other hand, if *no* away side trigger is required, typically all of the energy of the away side parton is lost to the medium [8,9]. Because the parton energy is on average roughly a factor of two more than the energy of the leading hadron, requiring a dihadron trigger reduces the signal strength of the shock wave by about a factor of six as compared to a single-hadron triggered event.

Let us now compare the strength of the shock wave correlation signal with next-to-leading and higher order fragmentation of the away side parton. For this comparison, we consider the associate momentum range of 1–2.5 GeV where the PHENIX collaboration has first seen indications for a shock wave [1]. As explained in detail in Refs. [9,11,12], we cannot reliably

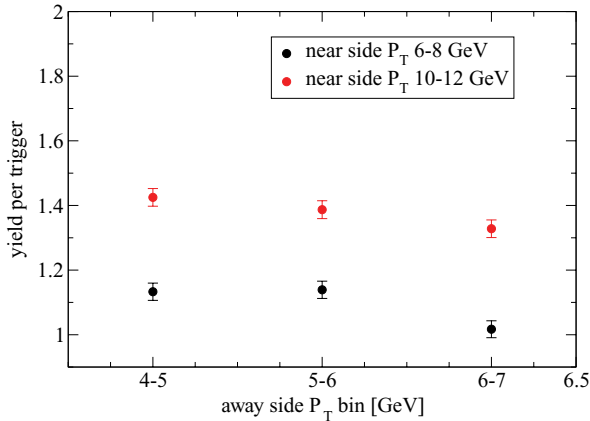


FIG. 2. (Color online) Estimated per-trigger yield of charged hadrons into the 1–2.5 GeV momentum bin due to subleading hadron production in fragmentation of the away side parton as a function of the near side and away side  $P_T$  range in central 200A GeV Au-Au collisions.

compute the precise magnitude of the shock wave per-trigger yield in a given momentum window, especially as long as the trigger is in a semihard regime below 6 GeV, as the yield is not only dependent on assumptions about flow in the medium, but also recombination/coalescence processes [26–28] need to be addressed below this scale. However, let us boldly assume that the per-trigger yield of charged hadrons in single-hadron triggered shock wave events scales with the average trigger momentum and based on this assumption extrapolate from the PHENIX data with a trigger of 2.5–4 GeV to the two fragmentation-dominated trigger ranges of 6–8 GeV and 10–12 GeV considered in this publication (note that there is good evidence from STAR data [4] that the rise of the yield is in fact substantially slower with trigger  $P_T$ ). With this maximal assumption, the per-trigger yield on the away side given the PHENIX acceptance in the 1–2.5 GeV associate momentum window for a 6–8 GeV trigger would be of order  $O(2.5)$  charged hadrons and for a 10–12 GeV trigger of order  $O(4)$  charged hadrons per trigger, and, again on the level of a rough approximation, reduced down to  $O(0.4)$  and  $O(0.7)$  in dihadron triggered events due to the bias on energy loss.

On the other hand, the per-trigger yield into the 1–2.5 GeV associate momentum window due to subleading fragmentation of the away side parton can be computed in our hadronization scheme using the approximations for  $A_3$  and  $A_4$  described above. The results are summarized in Fig. 2.

As seen from Fig. 2, the yield is chiefly determined by the highest momentum scale (i.e., the near side trigger momentum), which is natural given that this sets the overall energy available for hadron production in the jet. As the away side momentum scale is increased, the associated yield decreases. This is not unexpected, because requiring a larger

fraction of the parton momentum to end up in the leading hadron, less momentum is available for subleading hadrons.

However, the most striking result is that the expected per-trigger yields are of order  $O(1)$ ; i.e., they are in fact by about a factor two larger than the upper limit for the per-trigger yields caused by the medium recoil due to the shock wave. This means that if dihadron triggers are used to study shock wave production, the dominant signal at midrapidity where the away side trigger hadron is observed is not the shock cone, but rather hadrons produced in NL fragmentation processes of the trigger parton. The shock wave must then be observed as a correction to this signal. Most importantly, a splitting of the peak with a dip at zero degrees and strength at large angles is not expected under these conditions.

#### IV. SUMMARY

We have discussed the expected changes in the correlation pattern seen in a hydrodynamical momentum regime when one goes from single-hadron triggered events to dihadron triggered events. The main advantage of a dihadron trigger is that the rapidity of the away side parton is tightly constrained; thus a study of the medium recoil on the away side as a function of rapidity becomes meaningful. However, there are two effects that complicate the observation of the medium recoil substantially. First, by requiring a hard away side hadron, there is a significant bias toward events in which little or no energy is deposited into the medium. This reduces the energy available to excite a shock wave, and hence the strength of the correlation by at least a factor six.

Furthermore, once a hard away side hadron is detected, it is almost unavoidable that subleading, softer hadrons are created within the shower. This contribution is rather strong at low momenta and competes with the bulk recoil of the medium. We estimated here that it is at the position of the away side parton about a factor of two stronger than the medium recoil.

However, it is possible to eliminate the latter contribution because of its different shape in rapidity: While any shock wave signal is expected to be elongated in rapidity because of longitudinal flow, the jet cone due to fragmentation in vacuum would not be elongated at all. Thus, by observing associate hadron production displaced in rapidity from a hard dihadron trigger, a (weak) shock wave signal should become visible without any contamination from soft hadron production in the jet.

#### ACKNOWLEDGMENTS

I thank J. Ruppert and J. Rak for stimulating discussions and helpful comments. This work was financially supported by the Academy of Finland, Project 115262.

[1] S. S. Adler *et al.* (PHENIX Collaboration), Phys. Rev. Lett. **97**, 052301 (2006).

[2] A. Adare *et al.* (PHENIX Collaboration), Phys. Rev. Lett. **98**, 232302 (2007).

[3] J. Adams *et al.* (STAR Collaboration), Phys. Rev. Lett. **95**, 152301 (2005).

[4] M. J. Horner (STAR Collaboration), J. Phys. G **34**, S995 (2007).

- [5] J. Adams *et al.* (STAR Collaboration), Phys. Rev. Lett. **97**, 162301 (2006).
- [6] J. Casalderrey-Solana, E. V. Shuryak, and D. Teaney, Nucl. Phys. **A774**, 577 (2006).
- [7] T. Renk, Phys. Rev. C **74**, 024903 (2006).
- [8] T. Renk and K. J. Eskola, Phys. Rev. C **75**, 054910 (2007).
- [9] T. Renk and J. Ruppert, Phys. Rev. C **73**, 011901(R) (2006).
- [10] J. G. Ulery *et al.* (STAR Collaboration), Int. J. Mod. Phys. E **16**, 2005 (2007); J. G. Ulery, PoS, **LHC07**, 036 (2007).
- [11] T. Renk and J. Ruppert, Phys. Rev. C **76**, 014908 (2007).
- [12] T. Renk and J. Ruppert, Phys. Lett. **B646**, 19 (2007).
- [13] T. Renk and K. J. Eskola, Phys. Rev. C **77**, 044905 (2008).
- [14] J. Pumplin, D. R. Stump, J. Huston, H. L. Lai, P. Nadolsky, and W. K. Tung, J. High Energy Phys. 07 (2002) 012.
- [15] D. Stump, J. Huston, J. Pumplin, W. K. Tung, H. L. Lai, S. Kuhlmann, and J. F. Owens, J. High Energy Phys. 10 (2003) 046.
- [16] M. Hirai, S. Kumano, and T. H. Nagai, Phys. Rev. C **70**, 044905 (2004).
- [17] K. J. Eskola, V. J. Kolhinen, and C. A. Salgado, Eur. Phys. J. C **9**, 61 (1999).
- [18] I. Sarcevic, S. D. Ellis, and P. Carruthers, Phys. Rev. D **40**, 1446 (1989).
- [19] R. Baier, Y. L. Dokshitzer, A. H. Mueller, S. Peigne, and D. Schiff, Nucl. Phys. **B484**, 265 (1997).
- [20] U. A. Wiedemann, Nucl. Phys. **B588**, 303 (2000).
- [21] R. Baier, A. H. Mueller, and D. Schiff, Phys. Lett. **B649**, 147 (2007).
- [22] C. A. Salgado and U. A. Wiedemann, Phys. Rev. D **68**, 014008 (2003).
- [23] K. J. Eskola, H. Honkanen, H. Niemi, P. V. Ruuskanen, and S. S. Rasanen, Phys. Rev. C **72**, 044904 (2005).
- [24] T. Renk, Phys. Rev. C **70**, 021903(R) (2004).
- [25] G. Corcella *et al.*, J. High Energy Phys. 01 (2001) 010; arXiv:hep-ph/0210213.
- [26] R. C. Hwa and C. B. Yang, Phys. Rev. C **70**, 024905 (2004).
- [27] V. Greco, C. M. Ko, and P. Levai, Phys. Rev. C **68**, 034904 (2003).
- [28] R. J. Fries, B. Muller, C. Nonaka, and S. A. Bass, Phys. Rev. C **68**, 044902 (2003).